

# O(N) Models with Topological Lattice Actions <sup>\*</sup>

Wolfgang Bietenholz<sup>† a</sup>, Michael Bögli<sup>b</sup>, Urs Gerber<sup>a</sup>, Ferenc Niedermayer<sup>b,c</sup>,  
Michele Pepe<sup>d</sup>, Fernando G. Rejón-Barrera<sup>e</sup> and Uwe-Jens Wiese<sup>b</sup>

<sup>a</sup> *Instituto de Ciencias Nucleares, Universidad Nacional Autónoma de México  
A.P. 70-543, C.P. 04510 Distrito Federal, Mexico*

<sup>b</sup> *Albert Einstein Center for Fundamental Physics  
Institute for Theoretical Physics, Bern University  
Sidlerstrasse 5, CH-3012 Bern, Switzerland*

<sup>c</sup> *Institute for Theoretical Physics – HAS, Eötvös University  
Pázmány sétány 1/a, 1117 Budapest, Hungary*

<sup>d</sup> *INFN, Sezione di Milano-Bicocca, Edificio U2  
Piazza della Scienza 3, 20126 Milano, Italy*

<sup>e</sup> *Institute for Theoretical Physics, University of Amsterdam  
Science Park 904, Postbus 94485, 1090 GL Amsterdam, The Netherlands*

E-mail: [wolbi@nucleares.unam.mx](mailto:wolbi@nucleares.unam.mx)

A variety of lattice discretisations of continuum actions has been considered, usually requiring the correct classical continuum limit. Here we discuss “weird” lattice formulations without that property, namely lattice actions that are invariant under most continuous deformations of the field configuration, in one version even without any coupling constants. It turns out that universality is powerful enough to still provide the correct quantum continuum limit, despite the absence of a classical limit, or a perturbative expansion. We demonstrate this for a set of O(N) models (or non-linear  $\sigma$ -models). Amazingly, such “weird” lattice actions are not only in the right universality class, but some of them even have practical benefits, in particular an excellent scaling behaviour.

*31st International Symposium on Lattice Field Theory - LATTICE 2013  
July 29 - August 3, 2013  
Mainz, Germany*

<sup>\*</sup>We thank Janos Balog, Peter Weisz and Ulli Wolff for helpful communications.

This work was supported in parts by the *Schweizerischer Nationalfonds* (SNF), and by the Mexican *Consejo Nacional de Ciencia y Tecnología* (CONACyT), project 155905/10 *Física de Partículas por medio de Simulaciones Numéricas* and through the scholarship 312631 for graduate studies, as well as DGAPA-UNAM.

<sup>†</sup>Speaker.

## 1. Topological Lattice Actions

Lattice field theory usually starts by discretising some continuum Lagrangian, such as<sup>1</sup>

$$\mathcal{L}(\Phi(x), \partial_\mu \Phi(x)) \longrightarrow \mathcal{L}_{\text{lat}}(\Phi_x, [\Phi_{x+a\hat{\mu}} - \Phi_x]/a). \quad (1.1)$$

The couplings of a discrete derivative may also be spread somewhat beyond nearest neighbour sites but the continuum extrapolation of physical quantities coincides. This is due to *universality*: the universality class is determined by the dimension of space-time and by the symmetries of the order parameter fields. A condition is locality, *i.e.* the couplings should decay at least exponentially with the distance, and it is popular to tacitly assume that also the classical continuum limit should reproduce the continuum Lagrangian, *e.g.*  $\lim_{a \rightarrow 0} [\Phi_{x+a\hat{\mu}} - \Phi_x]/a = \partial_\mu \Phi(x)$ .

Here we investigate counter-examples to the last assumption, namely lattice actions which do not have any classical limit. Thus we are probing how far universality really reaches. It turns out that the quantum continuum limit may still be correct, and — surprisingly — such highly unconventional lattice formulations even have practical virtues.

We study O(N) models, with classical spins of unit length attached to each lattice site,

$$\vec{e}_x = (e_x^1, \dots, e_x^N), \quad |\vec{e}_x| = 1 \quad \forall x = na, \quad n \in \mathbb{Z}^d. \quad (1.2)$$

We consider the dimensions  $d = 1$  and  $2$ , and  $N = 2$  (XY model, relevant *e.g.* for superfluid <sup>4</sup>He films) and  $N = 3$  (classical Heisenberg model, asymptotically free, describes ferromagnets). For  $N = d + 1$ , periodic boundary conditions imply that the configurations occur in topological sectors (we employ the geometric definition of the topological charge of lattice configurations).

The simplest and most radical topological action is the *constraint action*, which just restricts the angles between all pairs of nearest neighbour spins by an upper bound  $\delta$ ,<sup>2</sup>

$$S[\vec{e}] = \sum_{\langle x,y \rangle} s(\vec{e}_x, \vec{e}_y), \quad s(\vec{e}_x, \vec{e}_y) = \begin{cases} 0 & \vec{e}_x \cdot \vec{e}_y > \cos \delta \\ +\infty & \text{otherwise} \end{cases}. \quad (1.3)$$

Most small deformations of a configuration (those within the allowed set) do not cost any action; this characterises *topological lattice actions*. All allowed configurations have the same action  $S = 0$ ; due to this enormous degeneracy, there is no classical limit, nor a perturbative expansion.

For models with topological charges  $Q = \sum_{\langle x,y,\dots \rangle} q_{\langle x,y,\dots \rangle}$  (where  $q$  is the topological charge density), we also consider the *Q suppressing action*

$$S[\vec{e}] = \lambda \sum_{\langle x,y,\dots \rangle} |q_{\langle x,y,\dots \rangle}|, \quad \lambda > 0. \quad (1.4)$$

The 2d XY model does not have topological sectors, but each plaquette carries a vortex number  $\nu_\square \in \{0, \pm 1\}$ , which can be suppressed analogously,  $S[\vec{e}] = \lambda \sum_\square |\nu_\square|$ .

We are going to consider constraint actions,  $Q$  (or vortex) suppressing actions, and combinations. All these are topological lattice actions, since  $S[\vec{e}]$  is invariant under most small deformations of the configuration  $[\vec{e}]$  (in contrast to lattice actions with discrete derivative terms).

<sup>1</sup>In this article, we do not consider gauge fields.

<sup>2</sup>O(N) model simulations with such a constraint have a pre-history, which includes Refs. [1].

## 2. The Quantum Rotor

The 1d XY model describes a quantum mechanical particle moving freely on a circle, with the continuum action  $S[\varphi] = \frac{I}{2} \int_0^\beta dt \dot{\varphi}(t)^2$  ( $\varphi(t)$ : angle,  $I$  moment of inertia). With periodicity,  $\varphi(\beta) = \varphi(0) \bmod 2\pi$ , this is the simplest model with topological sectors.

For the constraint action (the  $Q$  suppressing action) the continuum limit is attained as  $\delta \rightarrow 0$  ( $\lambda \rightarrow \infty$ ). The following table displays the asymptotic behaviour for two scaling terms [2].

scaling term	continuum	constraint action	$Q$ suppressing action
$\frac{E_2 - E_0}{E_1 - E_0}$	4	$4(1 + \frac{3}{5} \frac{a}{\xi} + \dots)$	$4(1 - \frac{3}{2} \frac{a}{\xi} + \dots)$
$\chi_t \xi = \frac{\langle Q^2 \rangle}{\beta(E_1 - E_0)}$	$\frac{1}{2\pi^2}$	$\frac{1}{2\pi^2}(1 - \frac{1}{5} \frac{a}{\xi} + \dots)$	$\frac{1}{2\pi^2}(1 + \frac{1}{2} \frac{a}{\xi} + \dots)$

The topological actions have *linear* scaling artifacts, which are unusual in scalar theories. However, the continuum values are consistently reproduced for  $a/\xi \rightarrow 0$  ( $\xi$ : correlation length,  $\chi_t$ : topological susceptibility). This is non-trivial; we do observe a facet of universality even in quantum mechanics, although universality is assumed to hold only in field theory,  $d \geq 2$ .

## 3. The 2d O(3) Model

The 2d O(3) model with coupling  $g$  (and periodic boundaries) has the continuum functionals

$$S[\vec{e}] = \frac{1}{2g^2} \int d^2x \partial_\mu \vec{e} \cdot \partial_\mu \vec{e}, \quad Q[\vec{e}] = \frac{1}{8\pi} \int d^2x \epsilon_{\mu\nu} \vec{e} \cdot (\partial_\mu \vec{e} \times \partial_\nu \vec{e}) \in \mathbb{Z}, \quad (3.1)$$

which obey the Schwarz inequality  $S[\vec{e}] \geq \frac{4\pi}{g^2} |Q[\vec{e}]|$  for each configuration.

On the *lattice*, the geometric topological charge takes the form  $Q[\vec{e}] = \frac{1}{4\pi} \sum_{\langle x,y,z \rangle} A_{x,y,z}$ , where  $x, y, z$  are corners of a triangle (half a plaquette), and  $A_{x,y,z}$  is the oriented area of the (minimal) spherical triangle spanned by  $\vec{e}_x, \vec{e}_y, \vec{e}_z$ . We consider the standard lattice action,  $S[\vec{e}] = -\frac{1}{g^2} \sum_{x,\mu} \vec{e}_x \cdot \vec{e}_{x+a\hat{\mu}}$ , the constraint action (1.3) and the  $Q$  suppressing action  $S[\vec{e}] = \lambda \sum_{\langle x,y,z \rangle} |A_{x,y,z}|$ .

As a scaling test we evaluated, on  $L \times 10L$  lattices, the step-2 Step Scaling Function (SSF) [3]  $\sigma(2, u_0) = 2L/\xi(2L)$ , with  $u_0 = L/\xi(L)$ . The continuum value  $\sigma(2, u_0 = 1.0595) = 1.26121$  [4] must be reproduced in the continuum extrapolation of simulation results with any lattice action in this universality class. For the constraint action, we performed precise numerical measurements with the Wolff cluster algorithm. Figure 1 (left) shows that the result is consistent with the continuum value. The data can be fitted to the same ansatz as the standard and modified actions,<sup>3</sup>

$$\Sigma(2, u_0, a/L) = \sigma(2, u_0) + \frac{a^2}{L^2} \left( c_1 \ln^3 \frac{a}{L} + c_2 \ln^2 \frac{a}{L} + \dots \right). \quad (3.2)$$

Amazingly, the constraint action even scales better than all the conventional actions included in Figure 1 (for them we took the data from Ref. [4]).

It has been predicted long ago that the “scaling term”  $\chi_t \xi^2$  diverges in the continuum limit of this model ( $\chi_t = \langle Q^2 \rangle / V$ ). A semi-classical argument refers to small topological dislocations,

<sup>3</sup>However, a recent discussion of O(N) models at large  $N$  suggests that the power of the leading logarithmic term might differ for the constraint action [5].

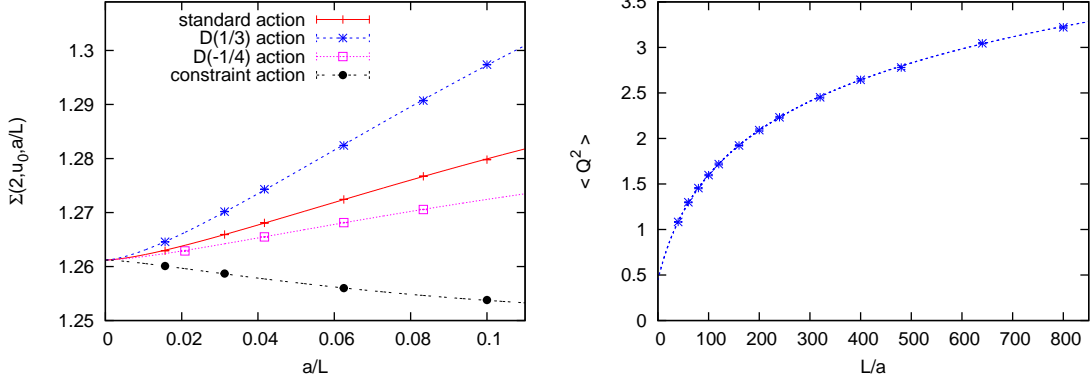


**Figure 1:** On the left: The step-2 SSF for the 2d O(3) model with  $u_0 = 1.0595$ , for four lattice actions. The constraint action has the correct continuum extrapolation, and the best scaling behaviour. On the right: The “scaling term”  $16\chi_t \xi_2^2 = \langle Q^2 \rangle$  diverges only *logarithmically* for the constraint action, although dislocations are not suppressed by any Boltzmann factor.

which are insufficiently suppressed [6]; that suggests a power divergence,  $\chi_t \xi_2^2 \propto (\xi/a)^p$ ,  $p \approx 0.9$ . Simulations with a (truncated) classically perfect action — which eliminates dislocations — revealed a logarithmic divergence [7].

The opposite extreme is the constraint action, which (for the nearly critical  $\delta$ -angles of interest) allows for dislocations without any action cost. To investigate its behaviour, we fixed<sup>4</sup>  $L/\xi_2 = 4$  and measured  $16\chi_t \xi_2^2 = \langle Q^2 \rangle$  as a function of  $L/a = 4\xi_2/a$ . The results for the constraint action (Figure 1, right) and for the  $Q$  suppressing action still diverge only logarithmically [2].

Due to this divergence, this model is sometimes considered “sick”, at least regarding topological properties. However, the correlation of the topological density,  $\langle q_x q_y \rangle$ , does have a regular continuum limit at non-zero separation [8],  $x \neq y$ , as we confirmed for the topological actions [2].

#### 4. The 2d XY Model

Here we can express the spins as  $\vec{e}_x = (\cos \varphi_x, \sin \varphi_x) \in S^1$ . For the relative angle between nearest neighbour spins we define the mod operation such that  $\Delta\varphi_{x, x+a\hat{\mu}} = (\varphi_x - \varphi_{x+a\hat{\mu}}) \bmod 2\pi \in (-\pi, \pi]$ . A plaquette  $\square$  with the corners  $x_1, x_2, x_3, x_4$  has the *vortex number*

$$v_\square = \frac{1}{2\pi} (\Delta\varphi_{x_1, x_2} + \Delta\varphi_{x_2, x_3} + \Delta\varphi_{x_3, x_4} + \Delta\varphi_{x_4, x_1}) \in \{0, \pm 1\}. \quad (4.1)$$

Periodic boundary conditions imply  $\sum_\square v_\square = 0$ .

For the standard action  $S[\vec{e}] = \beta \sum_{x, \mu} (1 - \vec{e}_x \cdot \vec{e}_{x+a\hat{\mu}})$  there is a well-known Berezinskii-Kosterlitz-Thouless (BKT) essential phase transition (of infinite order) at  $1/\beta_c = 1.1199(1)$  [9], where the correlation length diverges exponentially,

$$\xi(\beta \lesssim \beta_c) \propto \exp(\text{constant}/\sqrt{\beta_c - \beta}). \quad (4.2)$$

The established picture describes this transition by the vortex dynamics: at  $\beta > \beta_c$  they occur (mostly) in tightly bound vortex–anti-vortex pairs, which leads to a *massless phase*. As we decrease  $\beta$  below  $\beta_c$  these pairs unbind and “disorder” the system, so we enter the *massive phase*. The value of  $\beta_c$  has been estimated based on the action cost for isolated vortices (or anti-vortices) [10].

<sup>4</sup> $\xi_2$  is the second moment correlation length; it almost coincides with  $\xi$ , but is easier to measure. Its use was motivated in particular by the  $Q$  suppressing action, where we could not apply the cluster algorithm.

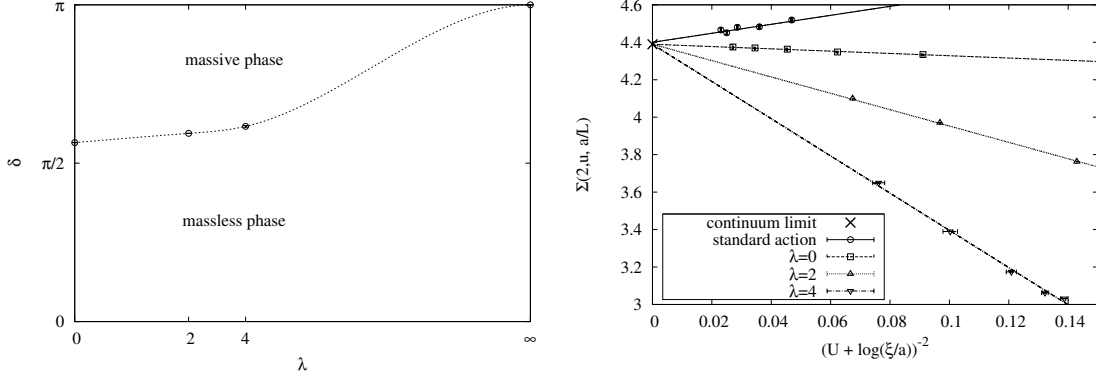


**Figure 2:** On the left: Schematic phase diagram for the 2d XY model with topological lattice actions. On the right: step-2 SSF for the standard action and three topological lattice actions, which are all compatible with the correct continuum extrapolation (for a suitable constant  $U$ ; the continuum value  $\sigma(2, 3.0038)$  is included in the fit). Also here the constraint action ( $\lambda = 0$ ) has a formidable scaling quality.

For the constraint action — with  $|\Delta\varphi_{x,x+a\hat{\mu}}| < \delta$  for all  $x, \mu$  — vortices are either excluded ( $\delta \leq \pi/2$ ), or allowed without any action cost. We simulated the constraint action, the vortex suppressing action  $S = \lambda \sum_{\square} |v_{\square}|$  and combinations (for  $\lambda > 0$  we elaborated a new variant of the cluster algorithm). At fixed  $\lambda = 0, 2$  or  $4$  we observed massive/massless phase transitions at [11]

$$\delta_c(\lambda = 0) = 1.7752(6), \quad \delta_c(\lambda = 2) = 1.8665(8), \quad \delta_c(\lambda = 4) = 1.936(8), \quad (4.3)$$

where the correlation length exhibits a BKT type divergence,

$$\xi(\delta \gtrsim \delta_c) \propto \exp(\text{constant}/\sqrt{\delta - \delta_c}). \quad (4.4)$$

The phase diagram is sketched in Figure 2 (left). In the vicinity of the transition, vortices are present (they are ruled out for  $\delta < \pi/2$  and  $\lambda = +\infty$ ). To probe the BKT behaviour further, we measured again the step-2 SSF, now referring to the continuum value  $\sigma(2, u = 2L/\xi(L) = 3.0038) = 4L/\xi(2L) = 4.3895$ , which had been confirmed for the standard action [12]. Figure 2 (right) shows those data, and our results for three topological actions, which are all compatible with a fit to the right continuum value. Again the constraint action (with  $\lambda = 0$ ) has an excellent scaling behaviour.

For that case, we further measured the dimensionless helicity modulus

$$\bar{\Upsilon} = -\partial_{\alpha}^2 \ln p(\alpha)|_{\alpha=0}, \quad (4.5)$$

where  $\alpha$  is a twist angle in the boundary conditions. The theoretical prediction at a BKT transition is  $\bar{\Upsilon}_c = 2/\pi$  [13]. We simulated with *dynamical boundary conditions* and determined  $\bar{\Upsilon}$  from the curvature in the histogram for the  $\alpha$  values [14]. Figure 3 on the left shows that for increasing volume a jump down to zero is approximated at  $\delta \gtrsim \delta_c$ , as expected. The plot on the right shows our results at fixed  $\delta_c$ , in various volumes, which we denote as  $\bar{\Upsilon}_c$ . Earlier studies dealt with the standard action [9] and the “step action” [15]. Those data are reproduced in our plot, but they confirmed the theoretical value only with a large  $L$  extrapolation. The standard action (step action) result at  $L = 2048$  ( $L = 256$ ) was still 5.6 % (4.1 %) off, whereas the constraint action results for  $L \geq 64$  match the prediction within the errors, and even down to  $L = 8$  they deviate only by 2.8 %.<sup>5</sup>

<sup>5</sup>If all these measurements were at a massless point, one would expect a universal curve  $\bar{\Upsilon}_c(L)$ . However, since one uses the parameters which would be critical in infinite volume, the correlation length is actually finite, and one obtains mixed finite size and lattice spacing artifacts, as usual.

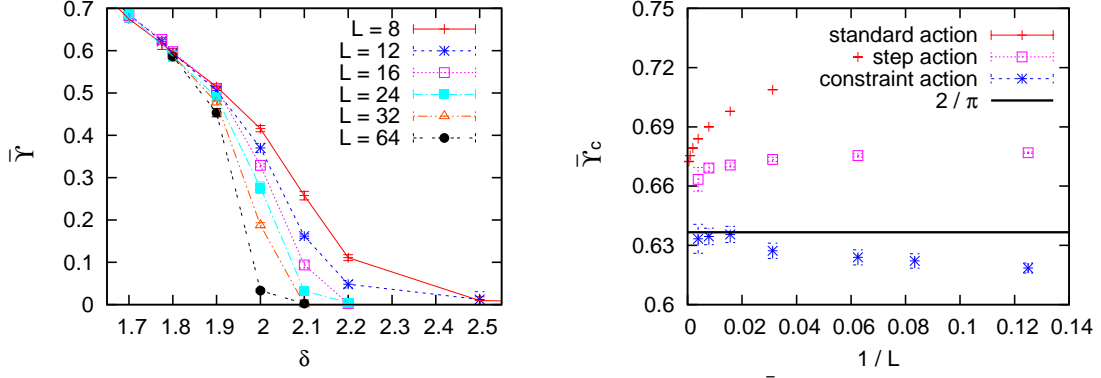


**Figure 3:** For the constraint action, the dimensionless helicity modulus  $\bar{\Upsilon}$  approaches a jump near  $\delta_c$  for increasing volume (on the left). At  $\delta_c$  it reproduces very well the BKT value  $2/\pi$  (on the right).

Finally we verified [14] that the (un)binding mechanism of vortex–anti-vortex pairs is still valid for this transition, even in the absence of any action cost for free vortices (and anti-vortices). Figure 4 (left) shows the densities of “free vortices”, defined as vortices which do not have an anti-vortex partner (or v.v.) within a distance of  $r = 1, 2$  or  $4$  lattice spacings. A significant density sets in as we increase  $\delta$  somewhat above  $\delta_c$ . Figure 4 (right) shows the “vorticity correlation function”

$$C(r) = \langle v_{\square,x} v_{\square,x+r} \rangle \Big|_{|v_{\square,x}|=1} . \quad (4.6)$$

In particular for  $r = 1$  — nearest neighbour pairs — we see a significant anti-correlation up to  $\delta \approx \delta_c$ , which fades away as we increase  $\delta$ . Along with measurements for the “optimal pair formation” (based on *simulated annealing*), we obtained compelling evidence that the (un)binding mechanism does indeed still drive the BKT transition, even for the constraint action [14].

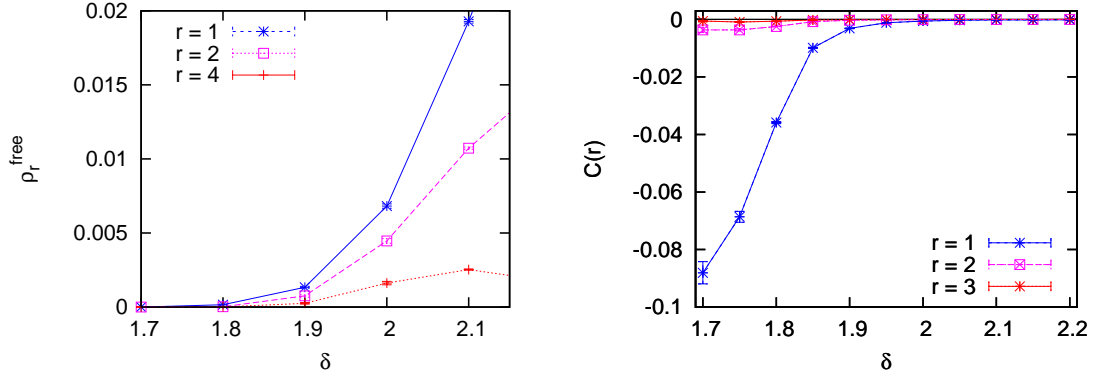


**Figure 4:** At  $\delta \gtrsim \delta_c$  the density of “free vortices” (without opposite partner within distance  $r$ ) rises (left), while the vorticity anti-correlation fades away (right). Both support the BKT (un)binding mechanism.

We return to the phase diagram in Figure 2 (on the left) and focus on the pure  $Q$  suppressing action (which corresponds to  $\delta = \pi$ ). Initially we expected the phase transition line to end somewhere on this upper axis at finite  $\lambda$ . However, the simulation results match  $\xi(\lambda) \propto \exp(0.729\lambda)$ , hence the endpoint is located at  $\lambda_c = +\infty$  (as depicted in the phase diagram) [11]. In this limit the vortices and anti-vortices are completely eliminated, so one may question whether this can still be a BKT transition. Indeed, the numerical result for the SSF [11],  $\sigma(2, u=6)_{\text{num}} = 9.47(1)$ , differs from the BKT value  $\sigma(2, u=6)_{\text{BKT}} = 11.53$  (provided by J. Balog). Therefore the transition at this endpoint is *not* of the BKT type; it belongs to another class, which has apparently been overlooked in the (tremendous) literature on this model.

## 5. Conclusions

Topological lattice actions do not have a classical limit, nor a perturbative expansion, but in the  $O(N)$  models studied here they do have the correct quantum continuum limit. This underscores the enormous power of universality. It even captures the *rotor* as a quantum mechanical model ( $d = 1$ ), though with unusual linear lattice artifacts.

In the  $2d O(3)$  model the constraint action violates the Schwarz inequality, but it has an excellent scaling behaviour, which can be further improved by a combination with a fine-tuned standard coupling constant [5]. The term  $\chi_i \xi^2$  diverges logarithmically in the continuum limit, but the correlator of the topological charge density,  $\langle q_x q_y \rangle$ , remains finite for  $x \neq y$ . This enabled precise studies of  $\theta$  vacuum effects [16].

In the  $2d XY$  model, the  $(\delta, \lambda)$  phase diagram has a BKT transition line at finite  $\lambda$  (at least up to  $\lambda = 4$ ). This was shown by measuring the SSF and the critical exponent  $\eta$  [11]. For the constraint action, the helicity modulus approaches a jump near  $\delta_c$  for increasing volume. At  $\delta_c$  it reproduces directly the BKT value  $\tilde{Y}_c = 2/\pi$ , which constitutes one of the best numerical evidences for a BKT transition. It is still driven by the vortex–anti-vortex pair (un)binding mechanism, now as a purely combinatorial effect, since there is no Boltzmann factor involved.

On the other hand, without a constraint angle, a new type of transition is attained at vortex suppression  $\lambda \rightarrow \infty$ ; this endpoint of the transition line in the  $(\delta, \lambda)$  phase diagram remains to be explored.

## References

- [1] W. Bietenholz, A. Pochinsky and U.-J. Wiese, *Phys. Rev. Lett.* **75** (1995) 4524. M. Hasenbusch, *Phys. Rev.* **D 53** (1996) 3445. A. Patrascioiu and E. Seiler, *J. Stat. Phys.* **106** (2002) 811.
- [2] W. Bietenholz, U. Gerber, M. Pepe and U.-J. Wiese, *JHEP* **1012** (2010) 020.
- [3] M. Lüscher, P. Weisz and U. Wolff, *Nucl. Phys.* **B 359** (1991) 221.
- [4] J. Balog, F. Niedermayer and P. Weisz, *Nucl. Phys.* **B 824** (2010) 563.
- [5] J. Balog, F. Niedermayer, M. Pepe, P. Weisz and U.-J. Wiese, *JHEP* **1211** (2012) 140.
- [6] M. Lüscher, *Nucl. Phys.* **B 200** (1982) 61.
- [7] M. Blatter, R. Burkhalter, P. Hasenfratz and F. Niedermayer, *Phys. Rev.* **D 53** (1996) 923.
- [8] S. Caracciolo, R.G. Edwards, A. Pelissetto and A.D. Sokal, *Phys. Rev. Lett.* **75** (1995) 1891.
- [9] M. Hasenbusch, *J. Phys.* **A 38** (2005) 5869.
- [10] J.M. Kosterlitz, *J. Phys.* **C 7** (1974) 1046.
- [11] W. Bietenholz, M. Bögli, F. Niedermayer, M. Pepe, F.G. Rejón-Barrera and U.-J. Wiese, *JHEP* **1303** (2013) 141.
- [12] J. Balog, F. Knechtli, T. Korzec and U. Wolff, *Nucl. Phys.* **B 675** (2003) 555.
- [13] D.R. Nelson and J.M. Kosterlitz, *Phys. Rev. Lett.* **39** (1977) 1201.
- [14] W. Bietenholz, U. Gerber and F.G. Rejón-Barrera, arXiv:1307.0485 [hep-lat].
- [15] P. Olsson and P. Holme, *Phys. Rev.* **B 63** (2001) 052407.
- [16] M. Bögli, F. Niedermayer, M. Pepe and U.-J. Wiese, *JHEP* **1204** (2012) 117. P. de Forcrand, M. Pepe and U.-J. Wiese, *Phys. Rev.* **D 86** (2012) 075006.